Equilibrium ion distribution in the presence of clearing electrodes and its influence on electron dynamics *

Georg H. Hoffstaetter, Christian Spethmann//CLASSE, Cornell University, Ithaca/NY 14850

Abstract

In an energy recovery linac (ERL) where beam-loss has to be minimal, and where beam positions and emittances have to be very stable in time, optic errors and beam instabilities due to ion effects have to be avoided. Possibly the least unattractive way of eliminating ions in an ERL is the installation of clearing electrodes. We present calculations of the remnant ion density and its effect on the beam.

INTRODUCTION

Ions can damage electron beams in various ways. It is therefore important to reduce the density of ions in the vicinity of the beam to a tolerable amount. Storage rings typically use ion-clearing gaps. These are short gaps in the filling pattern that lead to an absence of focusing forces for the ions every time this gap travels around the ring. The length of the beam-filled region and of the gap are chosen to overfocus ions and let them oscillate to large amplitudes out of the beam center. In pulsed linacs, the gaps are often long enough to allow ions to drift out of the beam region.

In rings with coasting beams, there is no ion-clearing gap, and obviously the beam cannot be turned off regularly. Similarly, in Energy Recovery Linacs (ERLs) [1] where the beam's energy is dumped in RF cavities and is immediately used to accelerate new electrons, one cannot easily turn off the beam (because this would interrupt the ERL process) and one can also not easily introduce short gaps in the beam (because this would disrupt the gun or the linac that injects large currents into the ERL). In both of these cases, ion-clearing electrodes may have to be used [2, 3].

The electron diameter varies along the accelerator, and this variation produces longitudinal forces, guiding ions to a location where the electron density is relatively large, typically close to the waists of the electron beam. Clearing electrodes are placed along the beam-line at such places of ion accumulation.

Because the motion to clearing electrodes that are spaced many meters apart takes several milliseconds, such electrodes tend to produce a linear ion density that is in the order of about one part in a thousand of the linear charge density in the beam.

Computing an equilibrium ion density is typically very time consuming. Here we use scaling properties of the Maxwell equations and the Lorentz force, as well as the adiabatic invariance of the action integral, to compute the equilibrium ion density very efficiently. We have applied this technique to analyze the Cornell ERL project [4].

* This work has been supported by NSF cooperative agreement PHY-0202078.

Table 1: Parameters of the Cornell ERL used for the examples in this paper.

Normalized emittances	$\varepsilon_{nx} = \varepsilon_{ny}$	$0.3 \cdot 10^{-6}$m
Energy spread	σ_δ	$2 \cdot 10^{-4}$
Electron current	I	0.1A
Bunch charge	Q	77pC
Injected energy	$E_{\rm in}$	10MeV
Top energy	$E_{\rm top}$	5GeV
Dominant ion abundance	H^+	98%
Ionization cross-section	$\sigma_{\rm col}$	$3.8 \cdot 10^{-23}$m^2
Gas density for warm sections	$p_{\rm line}$	$3 \cdot 10^{13}$m^{-3}
Gas density for cryogenic linac	$p_{\rm LINAC}$	$3 \cdot 10^{11}$m^{-3}

THE ION EQUILIBRIUM

For a rotationally symmetric electron beam, the density is given by

$$\rho_e(r,s) = \lambda \frac{1}{2\pi\sigma(s)^2} e^{-\frac{r^2}{2\sigma(s)^2}} . \qquad (1)$$

where λ is the linear particle density. With Gauss' law, the transverse velocity kick on a singly charged, non relativistic ion becomes

$$\Delta v_r = -\frac{2Ncr_p}{Ar}\left(1-\exp\left[\frac{-r^2}{2\sigma^2}\right]\right) , \qquad (2)$$

where σ is the rms width of the electron-beam profile, r is the distance from the beam centerline, N the number of electrons in the bunch, r_p the classical proton radius and A the atomic weight of the ion. The longitudinal kick in the special case of a round beam is given by [5]

$$\Delta v_s = -\alpha\varepsilon\left(\frac{\partial\,\Delta v_x}{\partial x} - \frac{\partial\,\Delta v_y}{\partial y}\right) . \qquad (3)$$

In a brute force simulation, the state of each ion is characterized by its x and s position, as well as by the velocities in both directions. Such a simulation would be very inefficient because there are two different timescales: A large number of kicks is required to resolve the sharply focused transverse ion motion, but the longitudinal motion hardly changes in a single oscillation. It is therefore not possible to simulate the motion of a realistic number of ions in this way.

During one transverse oscillation the longitudinal position s of the ion changes typically only by a fraction of a millimeter even at the largest possible ion speeds. Ions thus oscillate in a potential that slowly changes over many periods. Because of this, an ion's action integral over one oscillation period is an adiabatic invariant of the motion. In

our improved simulation, the state of the ion is therefore described by its longitudinal position s, its longitudinal speed v_s and its action integral J. Solving the motion in (J, s) rather than in (x, s) coordinates has two advantages: (1) The degrees of freedom are reduced from 2 to 1. (2) Because Δv_s changes much slower than Δv_x, the integration steps can be vastly increased, typically by about a factor of 10000. If the density at s is to be computed, it is not enough to know the action at s, but one oscillation is sufficient to compute the density contribution of particles with action J.

The longitudinal acceleration averaged over one oscillation is given by the time average over individual kicks. Calculating this time average again and again for each ion is computationally demanding and wasteful. Instead, we pre-compute a table of possible values of this time average for many beam sizes σ and amplitudes a of the oscillation.

The program was further accelerated by noting that the time averaged kick as a function of J can be calculated for a typical standard beam size and then rescaled for regions with other beam sizes,

$$\left\langle \frac{\partial\, \Delta v_x}{\partial x} + \frac{\partial\, \Delta v_y}{\partial y} \right\rangle = \frac{1}{\sigma^2}\, f(J/\sigma)\,. \tag{4}$$

This is due to scaling properties of the Maxwell equations [6]. The longitudinal acceleration of the ions is then given by

$$\dot{v}_s = -\frac{\alpha\varepsilon}{\sigma^2}\, f(J/\sigma)\,. \tag{5}$$

Ions are created with equal rate at all locations along the beam. Under the influence of the longitudinal beam force, the ions will then slowly propagate to the point with minimal potential. In our simulation, we assume that clearing electrodes have been placed at the waist, so that ions crossing the $s = 0$ line are removed. An equilibrium situation is reached when an equal number of ions are produced and removed during a given time interval.

Fig.1 shows one half of a L=12.6m long part of the beam with a waist of $\beta^* = 28.97$m at its center. There is a sharp increase in the ion density near the electrode at $s = 960.15$m

Close to the beam axis, the transverse ion density diverges approximately as $1/r$, so that it is not appropriate to fit the ion distribution to a Gaussian. The $1/r$ distribution leads to a constant radial electric field near the beam axis which strongly affects beam dynamics. As long as the number of ions per length is much smaller than the number of electrons per length the $1/r$ scaling of the ion density is not altered by ion-ion forces in by far the largest part of the beam [6].

ELECTRON MOTION WITH IONS

As a worst case scenario, we simulated a drift region with 200m length and a beam waist of $\beta^* = 100$m at the center. The final phase-space distribution with and without the ion field is shown in Fig. 2. While passing through the

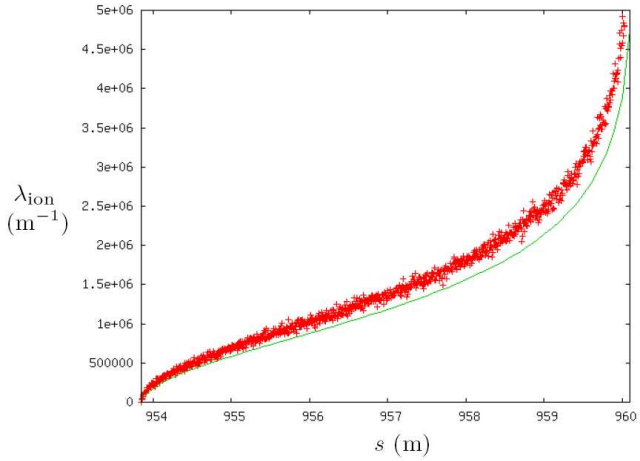

Figure 1: Simulated and analytically approximated linear ion densities near s=960m in the Cornell ERL.

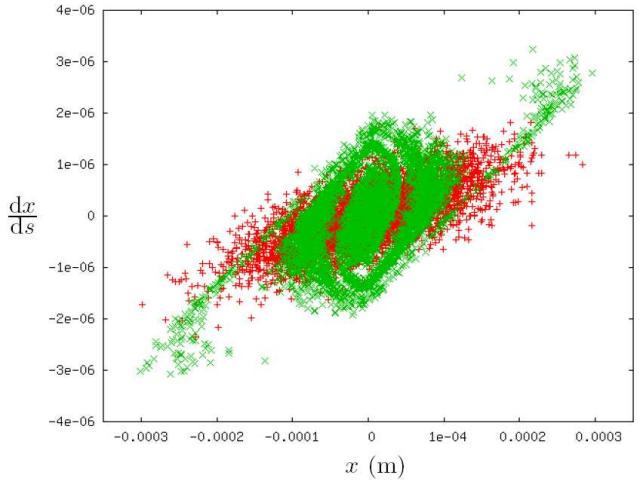

Figure 2: Electron beam phase-space distribution after transversing the 200m ion field with $\beta^* = 100$m at its center. Dark-red $+$: phase space in a free drift, Light-green $\times$: phase space for motion through the ion field.

ion field once, the beam emittance was found to increase from 36.6pm to 50.7pm.

This example shows that sections of only a few times 10 meters between clearing electrodes can produce intolerable emittance growth if the β-function is large. It therefore has to be tested whether the optics in the Cornell ERL provides fast enough ion motion to clearing electrodes, so that emittance growth is limited.

Because ions travel to the minima of the electrostatic potential, a clearing electrode has to be located at every such minimum. We therefore first calculate the potential in the beam's center. For this we used the potential in [7] which assumes a beam with uniform transverse charge density. Fig. 3 (top) shows the resulting potential in the center of the beam.

To find a round beam approximation suitable to our simulations, we first look at the minima of this potential and

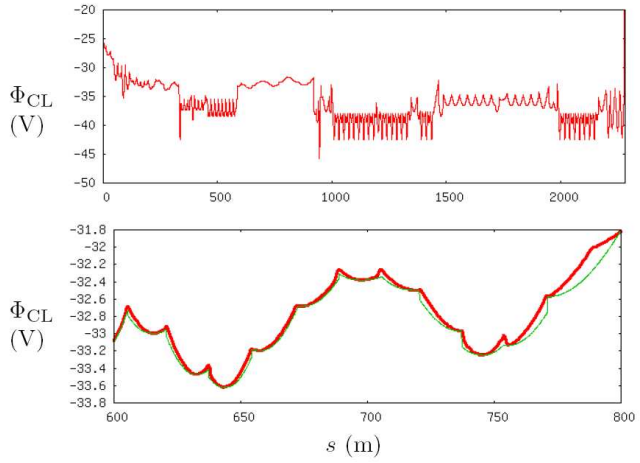

Figure 3: Top: Approximate longitudinal beam potential for the Cornell ERL. Bottom: A section of the ERL illustrating the approximation of the beam's potential (thick-dark-red) by a round-beam model (thin-light-green).

calculate the β-function that would give the same potential at those locations in the case of a round beam. We can then define a round beam approximation for the entire ERL lattice by using a free drift from one potential maximum to the next. Fig.3 (bottom) shows that this is a good approximation. The longitudinal ion velocities near the center of the beam (where most of the ions are located) depend only on this potential. Fig.1 shows that ions which are not in the center have the same velocity to a good approximation. This clearing speed determines the linear ion density also for non-round beams, and our round beam model should therefore be a good approximation.

Integrating over the relevant upstream points from the nearest potential maximum to s yields the total local ion density at s

$$\rho(s) = \int_{s_{\rm max}}^{s} \frac{\sigma I \rho_n(s_0)}{e} \frac{{\rm d}s_0}{\sqrt{\frac{2e}{m_{\rm ion}}\left[V(s_0) - V(s)\right]}} \,. \qquad (6)$$

Using this method, and assuming that the residual gas density in the linac sections is reduced by a factor 100 as specified in Tab. 1, we find the linear ion densities for the Cornell ERL shown in Fig. 4.

The example in Fig.1 represents the section of the ERL with the largest linear ion density. To reduce the impact of high density sections like this, additional clearing electrodes can be placed between the maximum and minimum of the potential. We find that by including one extra electrode, the emittance increase caused by this section can be reduced from 1.04pm to 0.46pm.

To get a better estimate of the ion effects in the full ERL, we also simulated the ion distribution in a 34m long region around $s = 1530$m, which corresponds to one of the medium high peaks in Fig. 4. Sending the beam through this section 1000 times results in the phase-space distribution in Fig. 5. We find that 6.2% of the beam electrons leave

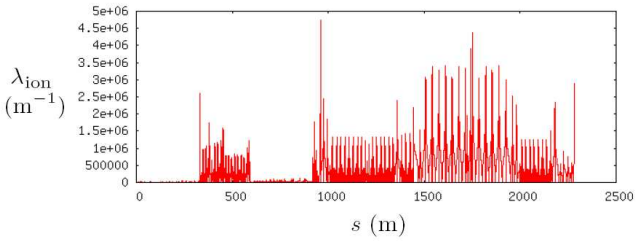

Figure 4: Estimate of the linear ion density at the Cornell ERL for a round beam approximation and clearing electrodes at the minima of the linear potential.

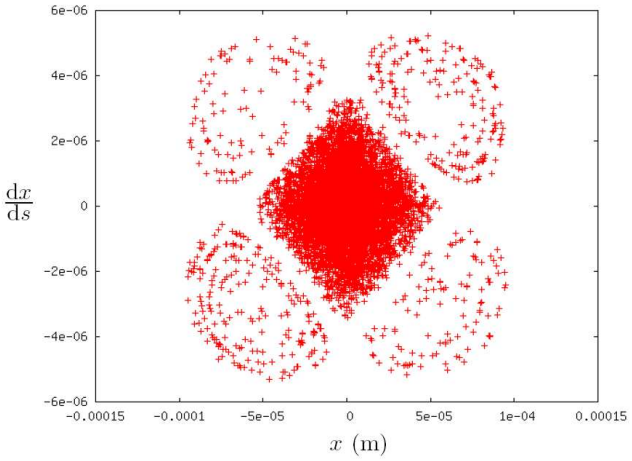

Figure 5: Electron beam phase-space plot after transversing a 34m long region with medium high ion density 1000 times.

the main bunch and migrate to the four separated islands in phase space.

REFERENCES

[1] G.H. Hoffstaetter, M.U. Liepe, Ion clearing in an ERL, NIM-A 557, p. 205 (2006)

[2] E. V. Bulyak, The ion core density in electron storage rings with clearing electrodes, in proceedings PAC93, Washington/DC (1993)

[3] E. V. Bulyak, Ion clearing methods for the electron storage ring, in proceedings EPAC96, Sitges/Spain (1996)

[4] G. H. Hoffstaetter, I.V. Bazarov, S. Belomestnykh, D.H. Bilderback, M.G. Billing, J.S-H. Choi, Z. Greenwald, S.M. Gruner, Y. Li, M. Liepe, H. Padamsee, D. Sagan, C.K. Sinclair, K.W. Smolenski, C. Song, R.M. Talman, M. Tigner, Status of a plan for an ERL extension to CESR, in proceedings PAC05, Knoxville/TN (2005)

[5] D. Sagan, Some aspects of the longitudinal motion of ions in electron storage rings, Nuclear Instruments and Methods in Physics Research A307 p. 171 (1991)

[6] G. Hoffstaetter, C. Spethmann, arXiv:0706.2897 (2007)

[7] E. Regenstreif, Potential and field created by an elliptic beam inside an infinite cylindrical vacuum chamber of circular cross-section, CERN/PS/DL 77-37 (1977)